Supporting Information for

Murine Calprotectin Coordinates Mn(II) at a Hexahistidine Site with Ca(II)-dependent Affinity

Rose C. Hadley[1], Derek M. Gagnon[2], Andrew Ozarowski[3], R. David Britt[2], and Elizabeth M. Nolan[1]*

[1]Department of Chemistry, Massachusetts Institute of Technology, Cambridge, MA 02139, USA

[2]Department of Chemistry, University of California, Davis, CA 95616, USA

[3] National High Magnetic Field Laboratory, Florida State University, Tallahassee, Florida 32310, USA

*Corresponding author: lnolan@mit.edu

Phone: 617-452-2495

This Supporting Information includes:

Design of the Synthetic Genes for mS100A8(H17A)(H27A), mS100A8(H83A)(H87A), mS100A9(H21A)(D31A), and mS100A9(H92A)(D96A)

The synthetic genes were optimized for *E. coli* codon usage and ordered from ATUM (formerly DNA2.0) in the pET41a vector. A *Nde*I restriction site was placed at the 5' end and a stop codon and a *Xho*I restriction site was placed at the 3' end (underlined below). Nucleotide sequences below are displayed from 5' to 3'.

Synthetic Gene for mS100A8(H17A)(H27A)

E. coli optimized nucleotide sequence for ***Nde*I**-mS100A8(H17A)(H27A)-Stop-***Xho*I**:

CAT ATG CCG AGC GAA CTG GAG AAA GCA CTG AGC AAC CTG ATC GAC GTC TAC GCG AAC TAC AGC AAT ATT CAA GGT AAT CAT GCG GCT CTG TAC AAA AAT GAT TTC AAG AAG ATG GTT ACC ACG GAG TGC CCG CAG TTC GTG CAG AAT ATC AAC ATT GAA AAC CTG TTC CGT GAG CTG GAC ATC AAC TCC GAT AAT GCC ATT AAC TTT GAA GAG TTT TTG GCG ATG GTT ATC AAA GTG GGC GTC GCG AGC CAC AAG GAC TCT CAT AAA GAG **TAA** CTC GAG

Translated sequence for ***Nde*I**-mS100A8(H17A)(H27A)-Stop-***Xho*I**:

M P S E L E K A L S N L I D V Y A N Y S N I Q G N H A A L Y K N D F K K M V T T E C P Q F V Q N I N I E N L F R E L D I N S D N A I N F E E F L A M V I K V G V A S H K D S H K E Stop **L E**

Synthetic Gene for mS100A8(H83A)(H87A)

E. coli optimized nucleotide sequence for ***Nde*I**-mS100A8(H83A)(H87A)-Stop-***Xho*I**:

CAT ATG CCG AGC GAA CTG GAG AAA GCA CTG AGC AAC CTG ATC GAC GTC TAC CAC AAC TAC AGC AAT ATT CAA GGT AAT CAT CAC GCT CTG TAC AAA AAT GAT TTC AAG AAG ATG GTT ACC ACG GAG TGC CCG CAG TTC GTG CAG AAT ATC AAC ATT GAA AAC CTG TTC CGT GAG CTG GAC ATC AAC TCC GAT AAT GCC ATT AAC TTT GAA GAG TTT TTG GCG ATG GTT ATC AAA GTG GGC GTC GCG AGC GCG AAG GAC TCT GCG AAA GAG **TAA** CTC GAG

Translated sequence for ***Nde*I**-mS100A8(H83A)(H87A)-Stop-***Xho*I**:

M P S E L E K A L S N L I D V Y H N Y S N I Q G N H H A L Y K N D F K K M V T T E C P Q F V Q N I N I E N L F R E L D I N S D N A I N F E E F L A M V I K V G V A S A K D S A K E Stop **L E**

Synthetic Gene for mS100A9(H21A)(D31A)

E. coli optimized nucleotide sequence for ***Nde*I**-mS100A9(H21A)(D31A)-Stop-***Xho*I**:

CAT ATG GCG AAC AAA GCA CCT AGC CAA ATG GAA CGC AGC ATC ACT ACT ATC ATC GAC ACT TTT GCG CAA TAC TCT CGT AAA GAG GGC CAC CCG GCG ACG CTG TCC

AAG AAA GAG TTC CGC CAG ATG GTT GAG GCC CAG CTG GCG ACC TTT ATG AAG AAA GAA AAA CGT AAC GAG GCA CTG ATT AAC GAC ATT ATG GAA GAT CTG GAC ACC AAT CAA GAT AAT CAG CTG AGC TTC GAA GAG TGC ATG ATG CTG ATG GCG AAG TTG ATT TTC GCT TGC CAC GAG AAG CTG CAT GAA AAC AAT CCG CGT GGT CAT GGT CAC AGC CAC GGT AAG GGT TGT GGC AAA **TAA** CTC GAG

Translated sequence for ***Nde*I**-mS100A9(H21A)(D31A)-Stop-***Xho*I**:

M A N K A P S Q M E R S I T T I I D T F A Q Y S R K E G H P A T L S K K E F R Q M V E A Q L A T F M K K E K R N E A L I N D I M E D L D T N Q D N Q L S F E E C M M L M A K L I F A C H E K L H E N N P R G H G H S H G K G C G K Stop **L E**

Synthetic Gene for mS100A9(H92A)(D96A)

E. coli optimized nucleotide sequence for ***Nde*I**-mS100A9(H92A)(H96A)-Stop-***Xho*I**:

CAT ATG GCG AAC AAA GCA CCT AGC CAA ATG GAA CGC AGC ATC ACT ACT ATC ATC GAC ACT TTT CAT CAA TAC TCT CGT AAA GAG GGC CAC CCG GAT ACG CTG TCC AAG AAA GAG TTC CGC CAG ATG GTT GAG GCC CAG CTG GCG ACC TTT ATG AAG AAA GAA AAA CGT AAC GAG GCA CTG ATT AAC GAC ATT ATG GAA GAT CTG GAC ACC AAT CAA GAT AAT CAG CTG AGC TTC GAA GAG TGC ATG ATG CTG ATG GCG AAG TTG ATT TTC GCT TGC GCG GAG AAG CTG GCG GAA AAC AAT CCG CGT GGT CAT GGT CAC AGC CAC GGT AAG GGT TGT GGC AAA **TAA** CTC GAG

Translated sequence for ***Nde*I**-mS100A9(H92A)(H96A)-Stop-***Xho*I**:

M A N K A P S Q M E R S I T T I I D T F H Q Y S R K E G H P D T L S K K E F R Q M V E A Q L A T F M K K E K R N E A L I N D I M E D L D T N Q D N Q L S F E E C M M L M A K L I F A C A E K L A E N N P R G H G H S H G K G C G K Stop **L E**

Mutations are highlighted in yellow.

Supporting Tables

Table S1. Compositions of murine calprotectin (mCP) variants.

Protein	mS100A8 subunit	mS100A9 subunit
mCP	mS100A8	mS100A9
mCPΔHis$_3$Asp	mS100A8(H83A)(H87A)	mS100A9(H21A)(D31A)
mCPΔHis$_4$	mS100A8(H17A)(H27A)	mS100A9(H92A)(H97A)
mCP(H103A)	mS100A8	mS100A9(H103A)
mCP(H105A)	mS100A8	mS100A9(H105A)
mCP(H107A)	mS100A8	mS100A9(H107A)
mCP(H103A)(H105A)	mS100A8	mS100A9(H103A)(H105A)
mCP(H103A)(H107A)	mS100A8	mS100A9(H103A)(H107A)
mCP(H105A)(H107A)	mS100A8	mS100A9(H105A)(H107A)
^{15}N-mCP	^{15}N-mS100A8	^{15}N-mS100A9

Table S2. Primers and templates for site-directed mutagenesis.[a]

Primer	Sequence	Template,[b] Temp.[c]
mA9(H103A)-1	5'-GAAAACAATCCGCGTGGT**GCT**GGTCACAGCCACGGTAAG-3'	*mA9*,
mA9(H103A)-2	5'-CTTACCGTGGCTGTGACC**AGC**ACCACGCGGATTGTTTTC-3'	60 °C
mA9(H105A)-1	5'-CAATCCGCGTGGTCATGGT**GCC**AGCCACGGTAAGGGTTGTG-3'	*mA9*,
mA9(H105A)-2	5'-CACAACCCTTACCGTGGCT**GGC**ACCATGACCACGCGGATTG-3'	61 °C
mA9(H107A)-1	5'-GGTCATGGTCACAGC**GCC**GGTAAGGGTTGTGGC-3'	*mA9*,
mA9(H107A)-2	5'-GCCACAACCCTTACC**GGC**GCTGTGACCATGACC-3'	66 °C
mA9(H103A)(H105A)-1	5'-GAAAACAATCCGCGTGGT**GCT**GGTGCCAGCCACGGTAAG-3'	*mA9(H105A)*,
mA9(H103A)(H105A)-2	5'-CTTACCGTGGCTGGCACC**AGC**ACCACGCGGATTGTTTTC-3'	63 °C
mA9(H103A)(H107A)-1	5'-GAAAACAATCCGCGTGGT**GCT**GGTCACAGCGCC-3'	*mA9(H107A)*,
mA9(H103A)(H107A)-2	5'-GGCGCTGTGACC**AGC**ACCACGCGGATTGTTTTC-3'	63 °C
mA9(H105A)(H107A)-1	5'-GTGGTCATGGTGCCAGC**GCC**GGTAAGGGTTGTG-3'	*mA9(H105A)*,
mA9(H105A)(H107A)-2	5'-CACAACCCTTACC**GGC**GCTGGCACCATGACCAC-3'	63 °C

[a] Bold codons indicate the mutation added. Underlined codons indicate a pre-existing mutation in the template plasmid relative to mS100A9. [b] The template plasmids are abbreviated by only including the name of the mS100A9 gene inserted between the *Nde*I and *Xho*I sites of pET41a. [c] Annealing temperature used in the PCR reaction.

Table S3. Mass spectrometry analysis of mCP subunits.[a]

Protein	mS100A8 subunit Calculated Mass ± ^{N}Met (Da)	Observed Mass (Da)[c]	mS100A9 subunit Calculated Mass ± ^{N}Met (Da)[b]	Observed Mass (Da)[c]
mCPΔHis$_3$Asp	10162.47 10031.28 (-Met1)[d]	10161.12 10031.10	12938.79 12807.60 (-Met1)[d]	n. f.[e] 12807.23
mCPΔHis$_4$	10162.47 10031.28 (-Met1)[d]	10162.11 10031.08	12916.74 12785.54 (-Met1)[d]	n.f.[e] 12784.77
mCP(H103A)	10294.59 10163.40 (-Met1)[d]	10294.16 10162.13	12982.80 12851.61 (-Met1)[d]	n. f.[e] 12851.17
mCP(H105A)	10294.59 10163.40 (-Met1)[d]	10293.15 10163.13	12982.80 12851.61 (-Met1)[d]	n. f.[e] 12851.19
mCP(H107A)	10294.59 10163.40 (-Met1)[d]	10293.15 10162.12	12982.80 12851.61 (-Met1)[d]	n. f.[e] 12851.29
mCP(H103A)(H105A)	10294.59 10163.40 (-Met1)[d]	10294.16 10163.13	12916.74 12785.54 (-Met1)[d]	n. f.[e] 12785.25
mCP(H103A)(H107A)	10294.59 10163.40 (-Met1)[d]	10294.16 10163.13	12916.74 12785.54 (-Met1)[d]	n. f.[e] 12785.23
mCP(H105A)(H107A)	10294.59 10163.40 (-Met1)[d]	10294.16 10163.13	12916.74 12785.54 (-Met1)[d]	n. f.[e] 12785.12
^{15}N-mCP	10416.65 10284.46 (-Met1)[d]	10415.77 10283.77	13213.64 13081.45 (-Met1)[d]	n. f.[e] 13079.95

[a] A denaturing protocol on an Agilent Poroshell 300SB-C18 column over a 25–75% gradient of acetonitrile with 0.1% formic acid was utilized for LC-MS. [b] Molecular weights were calculated by using the ProtParam tool found on the ExPASy site (http://web.expasy.org/protparam) with the exception of ^{15}N-mCP (http://sopnmr.ucsd.edu/biomol-tools.htm). [c] Masses were calculated with the Agilent MassHunter BioConfirm software package. [d] The N-terminal methionine can be cleaved during overexpression in *E. coli*. [e] Not found; the mass was not found following deconvolution of the raw data.

Table S4. Metal content of representative protein preparations.[a]

	mCP variant		
Metal	**mCP**[b] (24.0 μM)[c]	**ΔHis$_3$Asp** (6.0 μM)[c]	**ΔHis$_4$** (11.1 μM)[c]
[Mn] (μM)	0.002	0.001	0.002
equivalents[d]	0.000	0.000	0.000
[Fe] (μM)	0.098	0.012	0.072
equivalents[d]	0.004	0.002	0.007
[Co] (μM)	0.000	0.000	0.001
equivalents[d]	0.000	0.000	0.000
[Ni] (μM)	0.019	0.010	0.020
equivalents[d]	0.001	0.002	0.002
[Cu] (μM)	0.018	0.001	0.008
equivalents[d]	0.001	0.000	0.001
[Zn] (μM)	0.100	0.037	0.089
equivalents[d]	0.004	0.006	0.008

[a] Metal analysis (ICP-MS) was performed on purified proteins. [b] Reported previously in supporting ref. 1 and included here for comparison. [c] The concentration of protein in the ICP-MS sample. [d] The equivalents of metal relative to the mCP heterodimer.

Table S5. Metal content of representative protein preparations continued.[a]

	mCP variant (mS100A9 C-terminal tail variants)					
Metal	**(H103A)** (10.5 μM) [b]	**(H105A)** (9.1 μM) [b]	**(H107A)** (15.1 μM) [b]	**(H103A) (H105A)** (19.3 μM) [b]	**(H103A) (H107A)** (15.7 μM) [b]	**(H105A) (H107A)** (20.6 μM) [b]
[Mn] (μM)	0.003	0.000	0.002	0.001	0.026	0.000
equivalents[c]	0.000	0.000	0.000	0.000	0.002	0.000
[Fe] (μM)	0.084	0.046	0.047	0.044	0.120	0.045
equivalents[c]	0.008	0.005	0.003	0.002	0.008	0.002
[Co] (μM)	0.000	0.000	0.000	0.000	0.000	0.000
equivalents[c]	0.000	0.000	0.000	0.000	0.000	0.000
[Ni] (μM)	0.012	0.012	0.010	0.014	0.008	0.008
equivalents[c]	0.001	0.001	0.001	0.001	0.000	0.000
[Cu] (μM)	0.011	0.011	0.009	0.004	0.007	0.008
equivalents[c]	0.001	0.001	0.001	0.000	0.000	0.000
[Zn] (μM)	0.117	0.078	0.146	0.071	0.054	0.041
equivalents[c]	0.011	0.009	0.010	0.004	0.003	0.002

[a] Metal analysis (ICP-MS) was performed on purified proteins. [b] The concentration of protein in the ICP-MS sample. [c] The equivalents of metal relative to the mCP heterodimer.

Table S6. Analytical SEC elution volume and calculated molecular weights of proteins.

Protein[a]	[Ca(II)] (mM)	[Mn(II)] (mM)	V_e (mL)[b]	MW (kDa)
Ribonuclease A[c]	0	0	13.5	13.7
Carbonic anhydrase[c]	0	0	11.8	29
Ovalbumin[c]	0	0	10.8	44
Conalbumin[c]	0	0	9.9	75
mCP	0	0	12.1	25.8
	0	1	11.5	34.0
	25	0.1	11.4	35.6
(500 μM protein)	0	5	11.4	35.6
ΔHis_3Asp	0	0	12.0	27.0
	25	0	11.3	37.3
	0	1	12.0	27.0
	25	0.1	11.3	37.3
(500 μM protein)	0	5	11.3	37.3
ΔHis_4	0	0	12.0	27.0
	25	0	11.6	32.5
	0	1	12.0	27.0
(H103A)	0	0	12.1	25.8
	25	0	11.4	35.6
	0	1	11.3	37.3
(H105A)	0	0	12.1	25.8
	25	0	11.5	34.0
	0	1	12.0	27.0
(H107A)	0	0	12.1	25.8
	25	0	11.4	35.6
	0	1	12.0	27.0
(H103A)(H105A)	0	0	12.0	27.0
	25	0	11.3	37.3
(H103A)(H107A)	0	0	12.0	27.0
	25	0	11.4	35.6
(H105A)(H107A)	0	0	12.0	27.0
	25	0	11.4	35.6

[a] The mCP concentration was 100 μM, except where indicated otherwise. The elution buffer was 75 mM HEPES, 100 mM NaCl, pH 7.0 ± 25 mM Ca(II) and T = 4 °C. [b] The elution volume (V_e) corresponds to the maximum peak absorbance at 280 nm. [c] These four proteins were used to generate a calibration curve used to determine molecular weights for the mCP samples. The listed molecular weights are the known molecular weights used to generate the calibration curve.

Supporting Figures

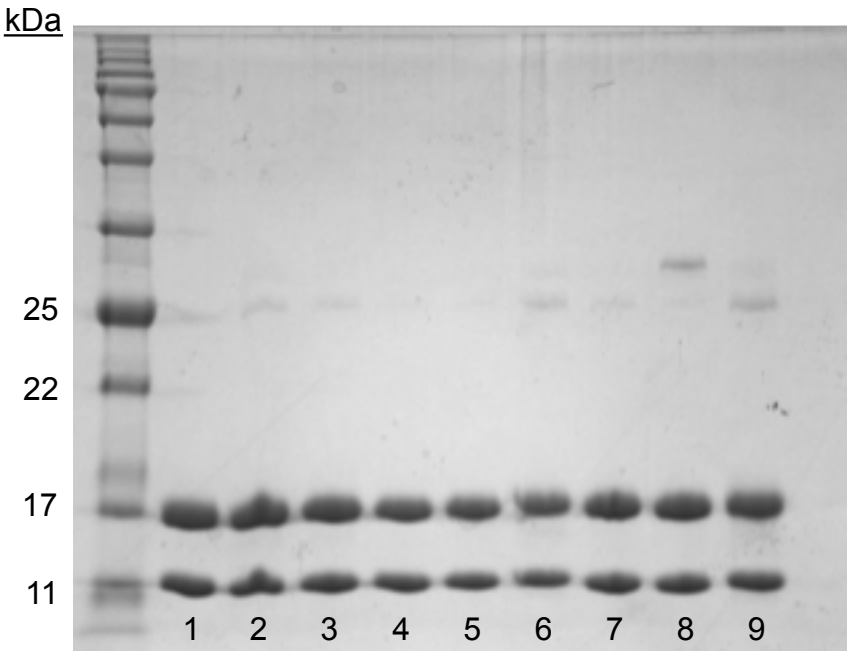

Figure S1. Purity of mCP variants by SDS-PAGE (15% Tris-glycine): (1) mCP(H103A), (2) mCP(H105A), (3) mCP(H107A), (4) mCP(H103A)(H105A), (5) mCP(H103A)(H107A), (6) mCP(H105A)(H107A), (7) mCPΔHis$_3$Asp, (8) mCPΔHis$_4$, (9) ^{15}N-mCP. The leftmost lane is a P7712S molecular weight ladder (New England Biolabs).

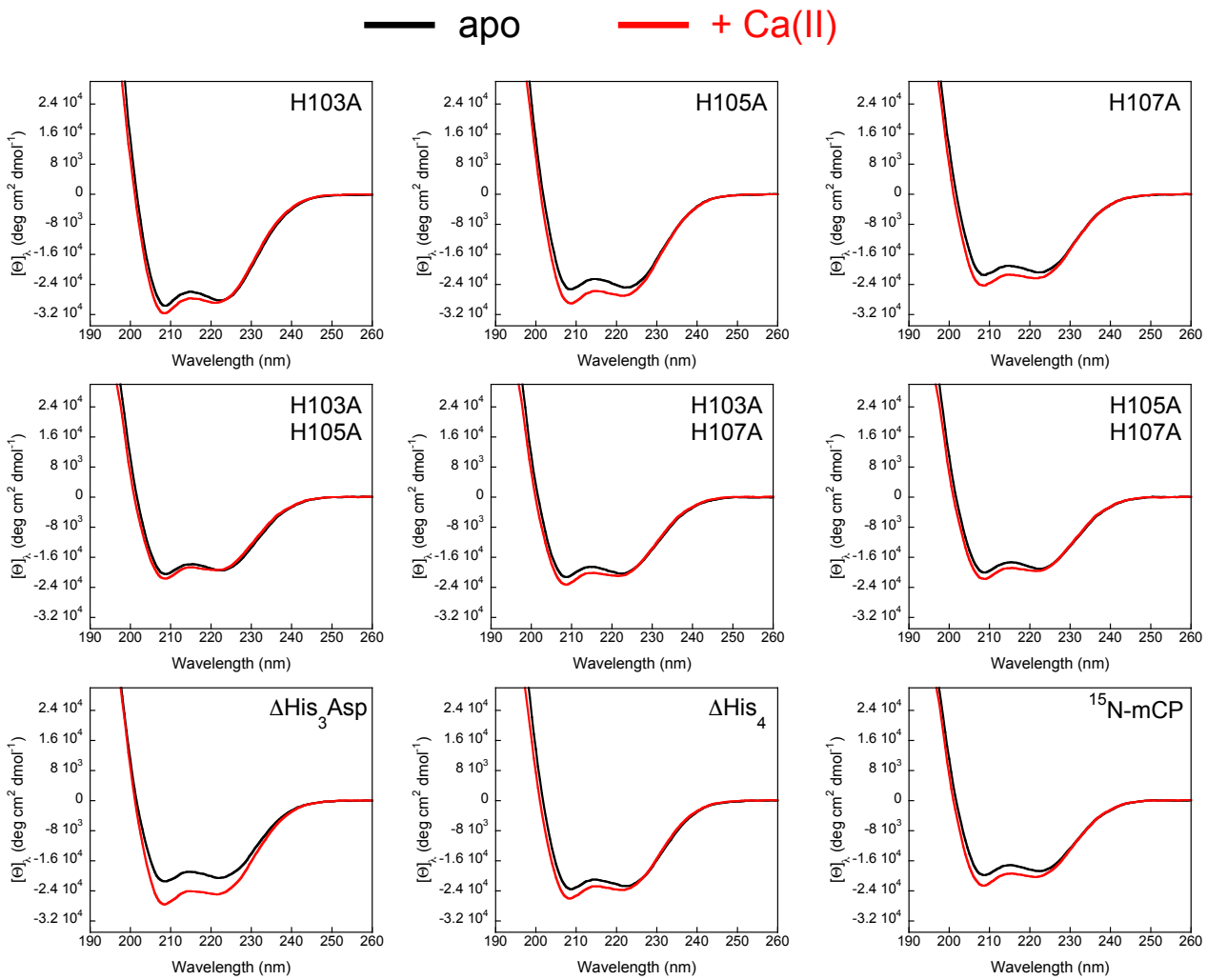

Figure S2. CD spectra of mCP variants (10 μM) in the absence (black) and presence (red) of 2 mM Ca(II) (1 mM Tris-HCl, 1 mM DTT, pH 7.5, T = 25 °C).

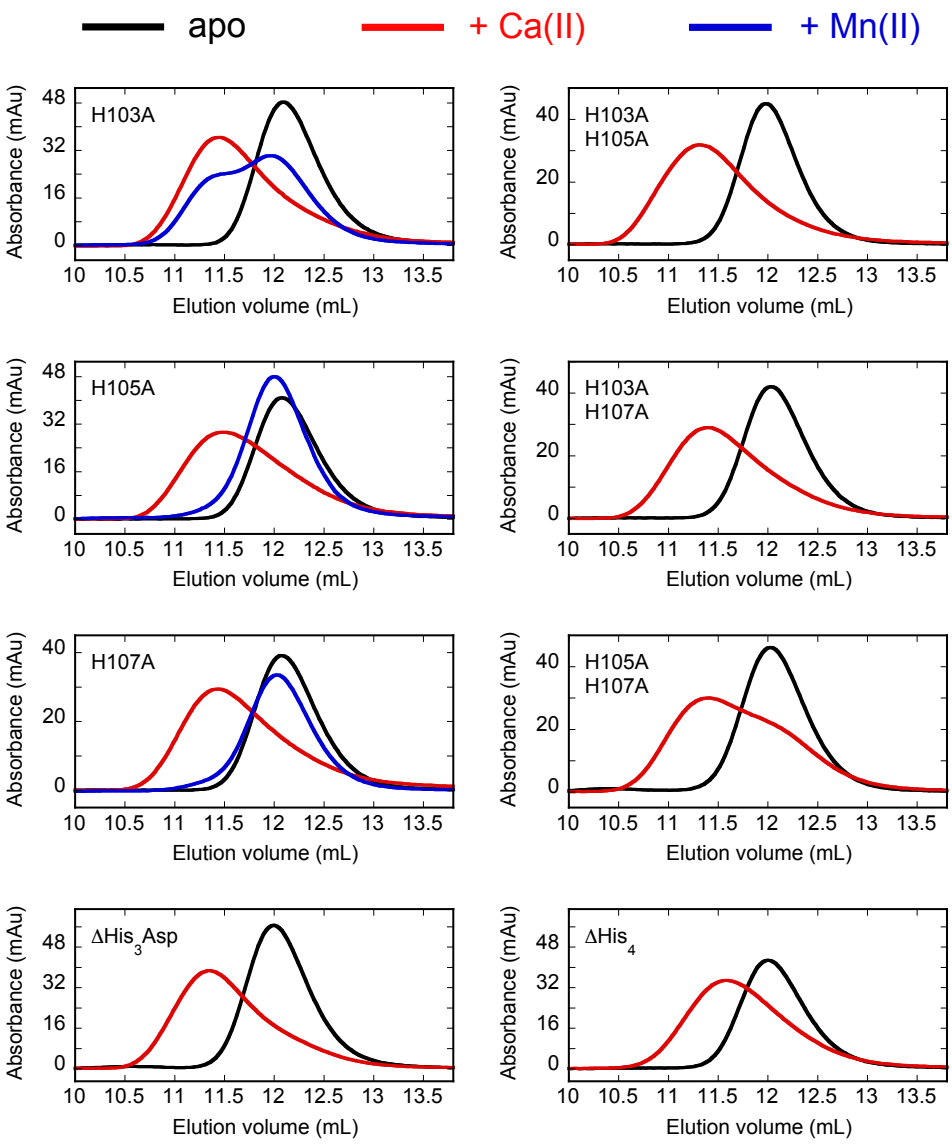

Figure S3. Analytical SEC chromatograms of mCP variants (100 μM) in the absence and presence of excess Ca(II). Single tail variants are also shown with 10 equiv Mn(II) in the sample and no Ca(II) added (blue traces) as a comparison. The buffer was 75 mM HEPES, 100 mM NaCl, pH 7.0, ± 25 mM Ca(II) in both the sample and elution buffer and T = 4 °C. Absorbance at 280 nm was monitored.

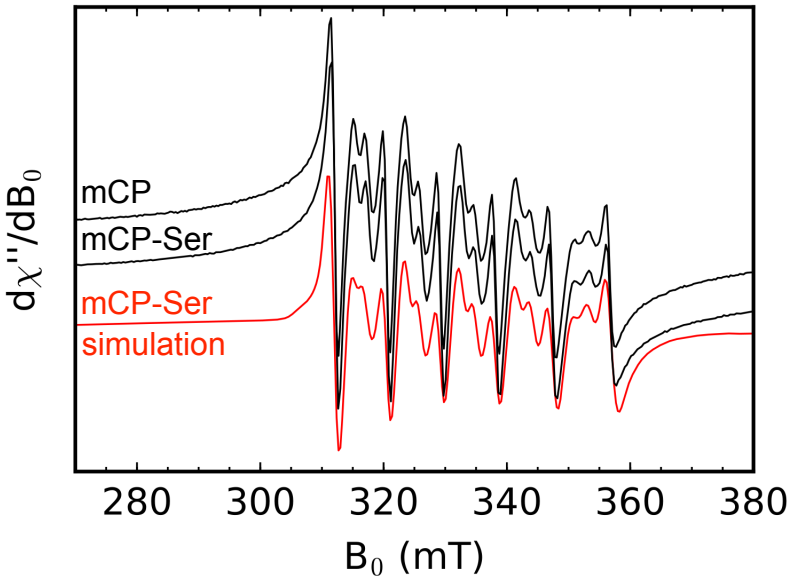

Figure S4. X-band EPR spectra of Mn(II)-bound mCP and mCP-Ser in the presence of excess Ca(II). The simulation of the mCP-Ser spectrum is shown in red. Experimental settings: temperature = 10 K, spectrometer frequency ≈9.38 GHz, modulation = 0.5 mT at 100 kHz, a data point was collected every ≈0.34 mT with an 80 ms conversion time, microwave power was 200 μW.

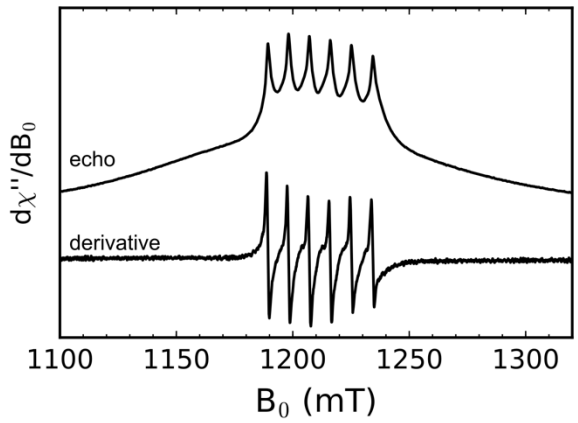

Figure S5. Echo detected Q-band field sweep of Mn(II)-bound mCP in the presence of excess Ca(II). The lower trace is the derivative of the upper, echo detected data. Experimental settings: temperature = 10 K, spectrometer frequency = 33.96 GHz, $\pi/2$ = 8 ns, a data point was collected every 0.1 mT, τ = 300 ns, shot repetition time = 1 ms.

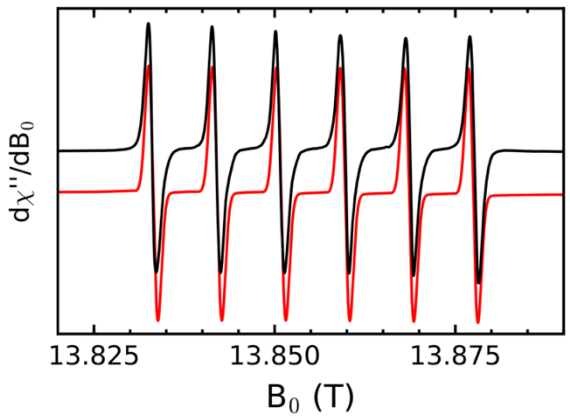

Figure S6. 388 GHz field sweep of Mn(II)-bound mCP in the presence of excess Ca(II) (black trace) and corresponding simulation (red trace). Temperature was 30 K, modulation amplitude of 0.5 mT at 50 kHz, and a sweep rate of 0.5 mT/s.

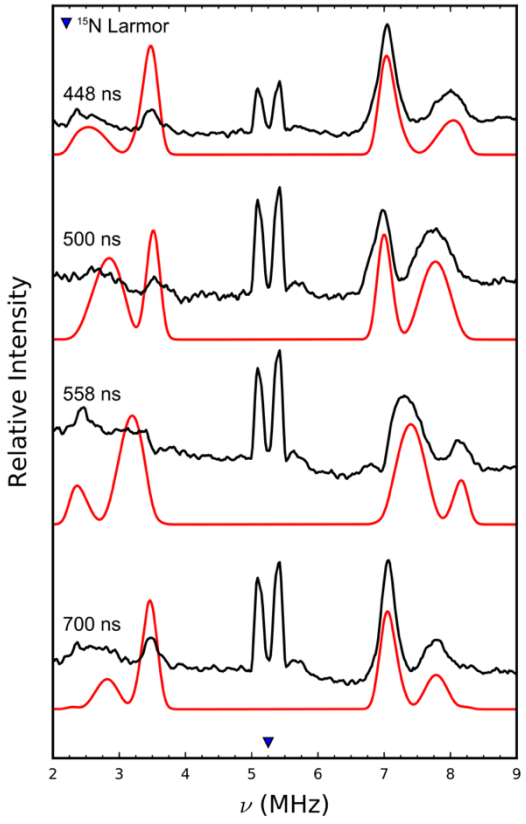

Figure S7. ^{15}N-Mims ENDOR spectra of globally ^{15}N-labeled Mn(II)-bound mCP in the presence of excess Ca(II) (black traces) collected at different τ values. The red traces are simulations. The numbers correspond to the τ value in ns. The inverted triangle indicates the ^{15}N Larmor frequency. Experimental settings: static field = 1216.6 mT, spectrometer frequency = 33.96 GHz, $\pi/2$ = 8 ns, delay between mw and RF pulses = 1 μs, RF pulse length = 50 μs, a point was collected every 19.5 kHz in stochastic mode, shot repetition time = 1 ms.

Example Simulation Code for Matlab R2017a and EasySpin

```
%% Example code for explicitly simulating a distribution in D-values, adapted from reference 2
clear
dta = dlmread('pre-processed_cwEPR_data.txt'); %load epr data in an easy to work with format
xe = dta(:,1);
ye = dta(:,2);

%Experiment
[~,~,params] = eprload('datafile.DTA'); % loads just the parameters from the experiment
%uses mw frequency recorded in Bruker parameter file and converts it to GHz%
Exp.mwFreq = params.MWFQ/10^9;
Exp.Range = [min(xe) max(xe)]; % mT
Exp.Temperature = 10;  % K
Exp.nPoints = length(ye);

% Generate all systems to be simulated, note only D is varied
D = 325:5:725; % MHz
for i = 1:length(D)
   Sys.S = 5/2;
   Sys.g = 2.0008;
   Sys.lw = [.7 0]; % mT
   Sys.Nucs = '55Mn';
   Sys.A = 248; % MHz
   Sys.D = [D(i) .30*D(i)];
   Sys.DStrain = [10 10]; % MHz
   Sys.HStrain = 42; % MHz
   Syss(i) = Sys;
   clear Sys
end
clear i

% Initializes a matrix to store individual simulations
ys = zeros(length(D),Exp.nPoints);
% Calculate spectra in parallel
parfor i = 1:length(D)
   [~,ys(i,:)] = pepper(Syss(i),Exp);
end
clear exp i

% Scale Simulated Spectra by Gaussian Distribution and Sum
ysc = zeros(size(ys));
prob = zeros(1,length(D));
sigma = 400/(2*sqrt(2*log(2)));
N = 1/(sigma*sqrt(2*pi));
D0 = (min(D)+max(D))/2;
for i = 1:length(D)
   prob(i) = N*exp(-(D(i)-D0).^2/(2*sigma^2));
   ysc(i,:) = prob(i)*ys(i,:);
end
clear i sigma N D0

ysim = zeros(1,length(ysc));
for i = 1:length(D)
   ysim = ysim+ysc(i,:);
end
```

Supporting Discussion on Simulation Methodology

Simulations of the X-band field sweeps required explicitly simulating each spectrum with several values of the axial zero-field splitting parameter *D* (see example code above) similar to a procedure previously used to simulate the EPR spectra of Mn(II)-bound human CP-Ser.[2] The simulations utilized an isotropic *g*-value, an isotropic ^{55}Mn hyperfine (a_{iso}), and values for the zero-field splitting parameters *D* and *E*. A two-step process was used to arrive at the reported simulation. First, rough values of the Hamiltonian parameters were fit by-the-eye using a modest *D* and *E* strain of 50 MHz, H strain of 42 MHz, and an isotropic convolutional Gaussian broadening of 0.7 mT. For a further explanation of the strains and isotropic convolutional broadening we refer the reader to the following resource: http://easyspin.org/easyspin/documentation/broadenings.html. We note that the isotropic convolutional broadening must be set sufficiently high for EasySpin to output the derivative EPR spectrum. These rough values were then used in simulations that explicitly loop over a range of *D* values ±200 MHz from the reported value. The E/D ratio was held constant at 0.30. A step size of 5 MHz was used for *D* and the *D* strain was reduced to 10 MHz.

The ^{15}N-Mims ENDOR was simulated using a simplified $S = ½$ spin system that did not include the ^{55}Mn hyperfine as was previously used for the ^{15}N-Mims ENDOR spectrum measured for Mn(II)-bound human CP-Ser.[2] This approximation was utilized since the pulse parameters and chosen field position bias the observed ^{15}N signals significantly towards transitions from m_s ±1/2 transition. The ^{15}N-Mims ENDOR simulations of distal and proximal nitrogen couplings were carried out utilizing only a single representative nitrogen for each class. Due to the apparent differences in the intrinsic ENDOR linewidths for the two classes of nitrogen atoms, we found it necessary to simulate each class (A and B in Figure 8 of the main text) separately, scale the results, and recombine the individual simulations for the two classes of nitrogen atoms. The proximal and distal nitrogen atoms were best simulated with ENDOR linewidths of 0.15 and 0.06 MHz, respectively. The hyperfine coupling parameters for the

nitrogen atoms were determined using a three-step process. At Q-band, the measured ^{15}N hyperfine couplings are in the "weak coupling" limit where a_{iso} is less than two times the Larmor frequency (5.25 MHz at 1.217 T). Therefore, the frequency difference of the two peaks provides a good first estimate of the isotropic coupling and the width of each signal provides an estimate of the anisotropic coupling. The second part of the process utilizes the estimated couplings as a starting point for the simulation which is then refined by-the-eye simultaneously for the four τ values collected. The third part of the process utilizes a least squares fitting implemented in the esfit fit function of EasySpin to further refine the simulations for each τ value. The final simulation is based on the average of the best fit for each τ value.

Supporting Reference

1. Hadley, R. C.; Gu, Y.; Nolan, E. M. Initial biochemical andfunctional evaluation of murine calprotectin reveals Ca(II)-dependence and its ability to chelate multiple nutrient transition metal ions. *Biochemistry* **2018**, *57*, 2846-2856.

2. Gagnon, D. M.; Brophy, M. B.; Bowman, S. E. J.; Stich, T. A.; Drennan, C. L.; Britt, R. D.; Nolan, E. M. Manganese binding properties of human calprotectin under conditions of high and low calcium: X-ray crystallographic and advanced electron paramagnetic resonance spectroscopic analysis. *J. Am. Chem. Soc.* **2015**, *137*, 3004-3016.